VI International Conference on Computational Methods for Coupled Problems in Science and Engineering
COUPLED PROBLEMS 2015
B. Schrefler, E. Oñate and M. Papadrakakis (Eds)

MULTI-PHYSICS AND MULTI-OBJECTIVE DESIGN OF A BENCHMARK DEVICE: A PROBLEM OF INVERSE INDUCTION HEATING

P. DI BARBA*, F. DUGHIERO†, M. FORZAN† AND E. SIENI†

* Department of Electrical, Computer and Biomedical Engineering
University of Pavia
27100 Pavia, Italy
e-mail: paolo.dibarba@unipv.it, web page: http://www. unipv.it

†Department of Industrial Engineering
University of Padova,
Via Gradenigo 6/a
35131 Padova, Italy
email: {fabrizio.dughiero,michele.forzan,elisabetta.sieni}@unipd.it - Web page: http://www.unipd.it

Keywords: induction heating, optimization, magnetic and thermal problem, multi-physics.

Abstract. In the paper, a bi-objective optimization problem characterized by a multi-physics field analysis is investigated. The optimal design of a pancake inductor, related to the design of industrial devices for the controlled heating of a graphite disk is considered as the benchmark problem. The expected goal of the optimization process is to improve temperature uniformity in the disk as well as electrical efficiency of the inductor. The optimized device is designed using a multi-physics problem: magnetic problem for electrical efficiency computation and thermal problem for temperature uniformity computation. The solution of the relevant bi-objective optimization problem is based on a modified multi-objective genetic algorithm in the class of Non-dominated Sorting Genetic Algorithm. The proposed algorithm exploits the migration concept to vary the population genetic characteristics during optimization process in order to improve the Pareto front approximation.

1. INTRODUCTION

Induction heating is used in thermal processes to heat the workpiece at a prescribed temperature with high efficiency and accurate temperature control. In this area the solution of coupled electromagnetic and thermal fields is mandatory, as well as the use of optimization algorithms to identify the best device [1–6].

In the paper, a benchmark model to approach a multiphysics bi-objective optimal design is presented [2–5,7–9]. A finite-element analysis (FEA) is used to solve the inverse problem, whereas the optimization is performed by means of a modified NSGA algorithm. The proposed optimization algorithm uses the migration concept [10–12] to vary the population genetic heritage in order to modify the Pareto front through a better approximation in the objective space. It is well known that the concept of migration is observable in nature when groups of people move to a new country and mix with local population. For instance, mathematical models of bio-geography inspired a class of derivative-free optimization

algorithms aiming to find an optimum balance between immigrating and emigrating populations in an island [10,13–17]. The concept of migration has been already implemented in other algorithms that make use of parallel computing. In these algorithms migration concept is referred to an exchange of individuals between independent islands that evolve autonomously [14,18–20]. In the proposed strategy the migration concept is used to modify the genetic characteristics of the current population.

The benchmark model represents an industrial device for the epitaxial processing of silicon wafer [2,7,9]. This device, meaningful from the industrial process viewpoint, has been already proposed as a test model for new optimization algorithms [2,3,5,7,9].

The designed device includes a graphite disk, a pancake inductor and a ferrite yoke. Since a pancake inductor does not induce power on the axis of the load, temperature close to the disk axis can be significantly lower. The magnetic concentrator is used to increase the induced power density and as consequence the temperature in the center of the disk.

The direct problem solves a time-harmonic magnetic problem to evaluate the power density in the graphite disk coupled to a steady-state thermal problem to evaluate the temperature profile.

2. PROBLEM DESCRIPTION

2.1. Direct problem

The 2D benchmark model, sketched in Figure 1 (a), includes a graphite disk with a radius of 357.5 mm, an inductor with 12 copper turns (a pancake inductor) and a ferrite ring, magnetic field concentrator, under the most internal turns (one or two) that are located at the same height. Moreover, the two most external turns are fixed at the same height. In Figure 1 (a) the design variables are also shown.

All turns, series connected, carry a current in the order of 500-600 A_{rms} at 4,250 Hz [7,21,22]. A total power of about 60 kW is prescribed in the device so that the disk reaches a steady state average temperature of 1050-1100 °C, as required by the industrial process. The corresponding inductor current is tuned in each FEA simulation: the FEA solution is updated with a new value of the inductor current (the source of electromagnetic model) when nonlinear material properties are taken into account in the model. Thermal and electrical properties of materials are in Table 1. In Figure 2, magnetic relative permeability and magnetization curve of the magnetic concentrator are presented.

The target of the multi-physics design is to evaluating the graphite disk temperature using a given inductor geometry. The magnetic analysis evaluates the power density in the graphite disk starting from the inductor geometry and the supply current. The power density is the source for the thermal problem.

The magnetic problem is solved in time-harmonic conditions by means of a commercial FEA code using the well-known **A**-V formulation, on second-order elements [23,24]. The current distribution in each turn is taken into account to correctly evaluate the inductor efficiency [2,25,26]. In particular, the magnetic problem is solved in terms of the phasor of the magnetic vector potential, $\boldsymbol{A}$ [2,3,25]:

$$\nabla^2 \dot{\boldsymbol{A}} - j\omega\mu\rho^{-1}\dot{\boldsymbol{A}} = -\mu\dot{\boldsymbol{J}} \tag{1}$$

where $\dot{\boldsymbol{J}}$ and $\dot{\boldsymbol{A}}$ are the phasors of the current density and magnetic vector potential, respectively, μ is the material magnetic permeability, ρ the material electrical resistivity and ω magnetic field pulsation. The resistivity depends on materials as reported in Table I and is the one of the graphite ($\rho=\rho_g$) in the disk, the one of the copper ($\rho=\rho_c$) in the inductor turns. Conductivity of the air and magnetic concentrator is null.

The electrical efficiency, η, is, then, computed from the power density as follow:

$$\eta = \frac{\int_{V_g} \rho_g^{-1} \omega^2 \left\| \dot{\boldsymbol{A}} \right\|^2 dV}{\int_{V_g} \rho_g^{-1} \omega^2 \left\| \dot{\boldsymbol{A}} \right\|^2 dV + \int_{V_c} \rho_c^{-1} \omega^2 \left\| \dot{\boldsymbol{A}} \right\|^2 dV} \tag{2}$$

where V_g and V_c are the volume of the graphite disk and the copper turns, respectively.

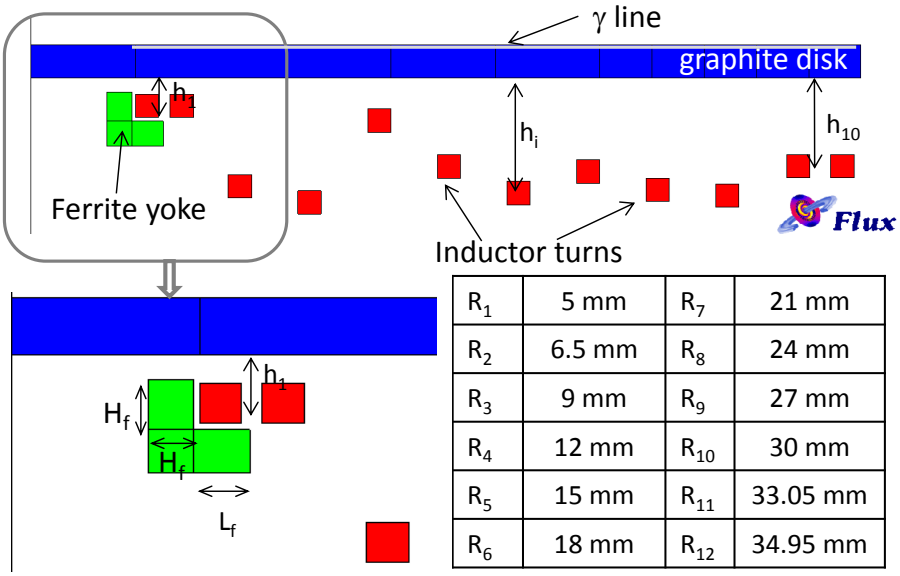

R_1	5 mm	R_7	21 mm
R_2	6.5 mm	R_8	24 mm
R_3	9 mm	R_9	27 mm
R_4	12 mm	R_{10}	30 mm
R_5	15 mm	R_{11}	33.05 mm
R_6	18 mm	R_{12}	34.95 mm

(a)

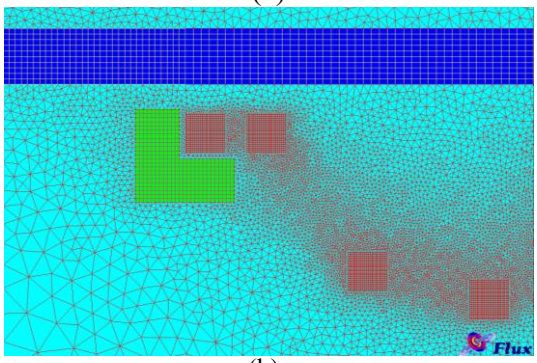

(b)

Figure 1: (a) Geometry of the benchmark model with 12 design variables. In the enlarged image the magnetic concentrator (ferrite ring), and the relevant design variables are also shown. Finally, in the table the radii of the turns are reported. (b) Detail of the mesh.

The thermal problem is solved in steady-state condition, assuming the power density in the disk computed by means of the magnetic problem as the source term [2,3,27]. The thermal

domain is the graphite disk. Along the domain profile a boundary condition of heat exchange along is imposed. The thermal conductivity of the graphite is reported in Table I [2,28,29]. From these assumptions, it results that the solutions of magnetic and thermal problem are weakly coupled by means of the source term of thermal equation:

$$-\nabla\cdot(\lambda\nabla T)=\rho^{-1}\omega^2\left\|\dot{\boldsymbol{A}}\right\|^2 \tag{3}$$

in which λ is the thermal conductivity of the material. Along the disk surface these boundary conditions subsist:

$$\frac{\partial T}{\partial n}=0 \tag{4}$$

at r = 0, and

$$-\lambda\frac{\partial T}{\partial n}=h\left(T-T_0\right)+\varepsilon k_B\left(T^4-T_0^4\right) \tag{5}$$

elsewhere, where h is the convective exchange coefficient (h=10 $Wm^{-2}K^{-1}$), ε emissivity coefficient (ε=0.6) and k_B Stefan-Boltzmann constant. The external temperature, T_0, is equal to 850 °C. These parameters of the thermal model have been tuned in order to fulfill experimental results of a real device considering that the expected average temperature is 1050-1100 °C.

Table 1: Electrical and thermal material properties of model materials

Element	**Electrical properties**		
Disk	Graphite (at 1200°C)	ρ_g=7.76 10^{-6} Ωm	μ_r = 1
Inductor	Copper	ρ_c=1.6 10^{-8} Ωm	μ_r = 1
Ferrite ring	Ferrite	--	Nonlinear. Relative permeability in Figure 2
	Thermal properties		
Disk	Graphite	λ=60 $Wm^{-1}K^{-1}$	

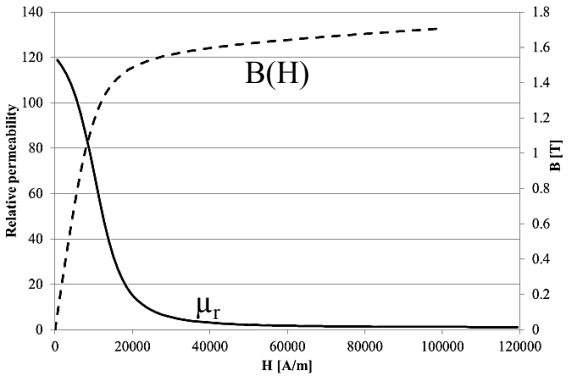

Figure 2: Relative permeability and magnetization curve of ferrite ring material.

A typical second-order mesh to solve the magnetic problem has 124,000 nodes and 57,000 elements. An example of the domain mesh is in Figure 1(b). The mesh of the thermal model is the one of the ferrite disk. The temperature has been evaluated on 201 sample points,

regularly spaced along the γ line showed in Figure 1(a).

2.2. Inverse problem

A 12-dimensional vector $\boldsymbol{x}$ of geometric design variables has been defined for the model in Figure 1 (a); the list of considered design variables with corresponding variation ranges is in Table 2. In particular, the design variables are the vertical positions of the inductor turns and the size of the magnetic yoke. The design problem is characterized by two conflicting objectives: the maximization of the electrical efficiency, η, defined as the ratio of active power transferred to the disk to the one transferred to the entire device using (2), and maximization of the temperature uniformity along the surface of the graphite disk at thermal steady state. In practice the inverse problem has been implemented as the simultaneously minimization of the following two objective functions:

$$f_1(\boldsymbol{x}) = 1 - \eta(\boldsymbol{x}) \tag{6}$$

$$f_2(\boldsymbol{x}) = \left[N_{\max} - \sup_j N_j(|T_j(\boldsymbol{x},\gamma) - T_i(\boldsymbol{x},\gamma)| < \frac{\Delta T^*}{2}) \right], \quad j \neq i \tag{7}$$

where f_1 is the complementary value of the electrical efficiency and f_2 measure the temperature in-homogeneity using the "criterion of proximity" [2,4,30]. This criterion is based on a tolerance interval, ΔT (=10°C), around a give temperature value. In practice for each solution the greatest number of points included in the tolerance band is searched for (that corresponds to search for the minimum number of points outside the tolerance band). A detailed description of this criterion is in [2,4,30]. An example of 'proximity criterion' is in Figure 3: considering the reference path γ, shown in Figure 1(a), 9 points satisfy the criterion while 14 points are outside the tolerance band ΔT; therefore 14 is the value assigned to f_2.

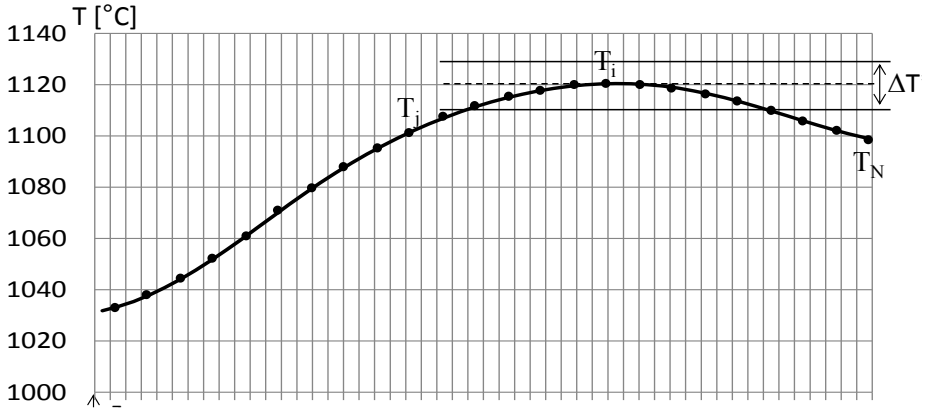

Figure 3: Example of "criterion of proximity" applied to the temperature along the γ path shown in Fig 1(a).

Table 2: Design variable ranges

	min	**max**
h_1,....., h_{10} [mm]	0	60
L_f [mm]	1	40
H_f [mm]	10	25

In the optimization problem, both functions (6) and (7) have to be minimized with respect to design variables shown in Figure 1 (a) and Table 2: the objective (6) refers to the magnetic domain, while the (7) refers to the thermal domain and a multi-physics and multi-objective inverse problem is originated.

1.1. Multi-physics optimization problem

The direct and inverse problems are coupled as in Figure 4 in order to create an optimization tool to design the improved geometry of the device in Figure 1(a). The multi-physics problem includes the solution in two steps of a magnetic problem and a thermal problem. The magnetic problem step includes two solutions of the same geometry if non-linear material properties are considered. The first solution is used to evaluate the amplitude of the current source in order that the power dissipated by the device is close to the prescribed one (e.g. 60 kW); whereas the power density that is the source term of the thermal problem, and the electrical efficiency that is the input of the optimization algorithm, are evaluated from the second solution. From the thermal problem the second input for the optimization algorithm, the temperature uniformity, is evaluated. Then, the solution of the multi-physics direct problem in terms of electric efficiency and temperature uniformity are the inputs of the optimization algorithm that generates a new set of design variables vectors.

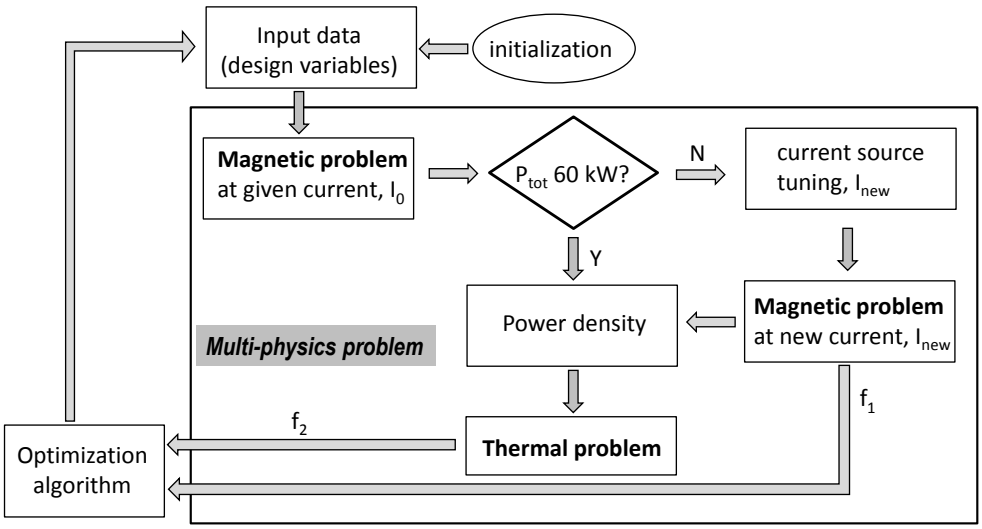

Figure 4 Coupling of the direct and inverse problem.

2. OPTIMIZATION ALGORITHM

Optimization process uses a modified NSGA-II algorithm, named Migration-NSGA, MNSGA, that implements the concept of the migration of groups of individuals that belong to populations with different genetic characteristics [8,31,32]. This algorithm mimics the event of the arrival of a group of individuals that mixes with the current population and has different characteristics with respect to originating population. The new individuals carry different genes that can improve the original population. This way, the genetic heritage of the population can be mutated.

MNSGA with the strategies sketched in Figure 5. A group of P_m individuals, generated

through a random process like the one applied to create the initial population, the 'immigrated population', is added to the current population after the main genetic operator (i.e. cross-over + mutation) and before the selection operator. This way, the immigrant individuals are added to the existing population of parents and off-springs and selection operates in such a way that, among the new individuals, only the ones with better characteristics are preserved in the population survived after selection.

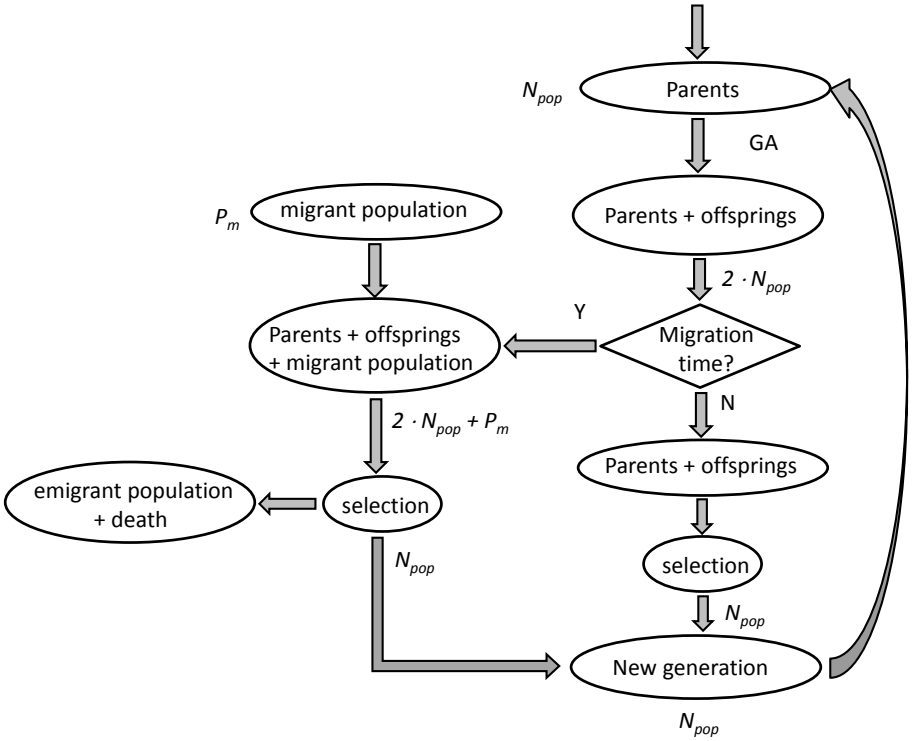

Figure 5 MNSGA algorithm

The concept of the population migration in a population with N_{pop} individuals is ruled by two parameters:

- the period of migration, T_m, with respect to the number of generations, corresponding to the number of iterations (e.g. T_m=1 is equivalent to introduce a migration at every iteration)
- the number of individuals in the immigrated population, P_m, between 1 and N_{pop}.

The number of individuals after selection is maintained constant to N_{pop} by applying natural selection and emigration events. Both the steps that reduce the population dimension managed in the selection algorithm intended as: a subgroup of individuals dies and a subgroup emigrates. In both cases some individuals come out from the population during the selection step of the NSGA algorithm.

3. RESULTS

The device in Figure 1(a) has been optimized using both standard NSGA-II and new MNSGA algorithm. In the MNSGA algorithm different values for the migration parameters, T_m and P_m, have been chosen (Table 3). The number of iterations of both algorithms, NSGA-

II and MNSGA, has been fixed to 50 with a population of 20 individuals. In Table 3 the maximum number of new individuals evaluated in each case during the optimization process is reported. It is evident that MNSGA algorithm evaluates a higher number of individuals and therefore implies an increased number of calls to the objective functions. Nevertheless, the increment of number of individuals in the order of 10-25 % improves the Pareto front approximation including more solutions that are not found using NSGA-II algorithm.

Table 3: Description of the optimization algorithm set-up.

#case	T_m	P_m	#NSGA-generated individuals	#immigrated individuals (increment[%])	#total individuals
NSGA	--	--	1020	--	1020
MNSGA_T2N10	2	10	1020	250 (+25%)	1270
MNSGA_T5N10	5	10	1020	100 (+10%)	1120
MNSGA_T5N20	5	20	1020	200 (+19%)	1220

In Figure 6 the comparison of the Pareto front for the cases NSGA and MNSGA_T5N20 (Table 3), obtained starting from the same initial population, is reported. The Pareto fronts found using MNSGA algorithm are broader with respect to the ones obtained using NSGA-II algorithm. Moreover, in some cases solutions found with NSGA-II are dominated by the ones obtained using MNSGA. It appears that the inclusion of new individuals (i.e. the immigration event) during the population evolution improves substantially the approximation of the Pareto front.

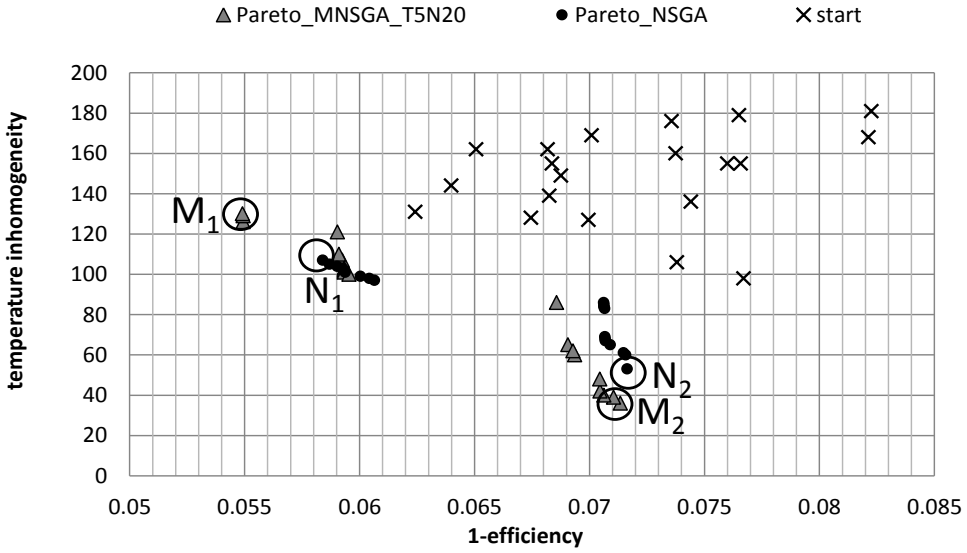

Figure 6 Starting populations and Pareto fronts obtained using NSGA-II and MNSGA algorithm.

Figures 7 and 8 show the geometries corresponding to the solutions outlined on the approximated Pareto front in Figure 6 and reported in Table 4. They have been obtained using NSGA-II algorithm and MNSGA algorithm, respectively. In each figure the solution of magnetic problem is shown in terms of the magnetic flux lines, whereas the thermal problem solution is shown in terms of the temperature along the disk profile. The difference in terms of temperature uniformity for the two solutions at the two ends of the Pareto front is evident.

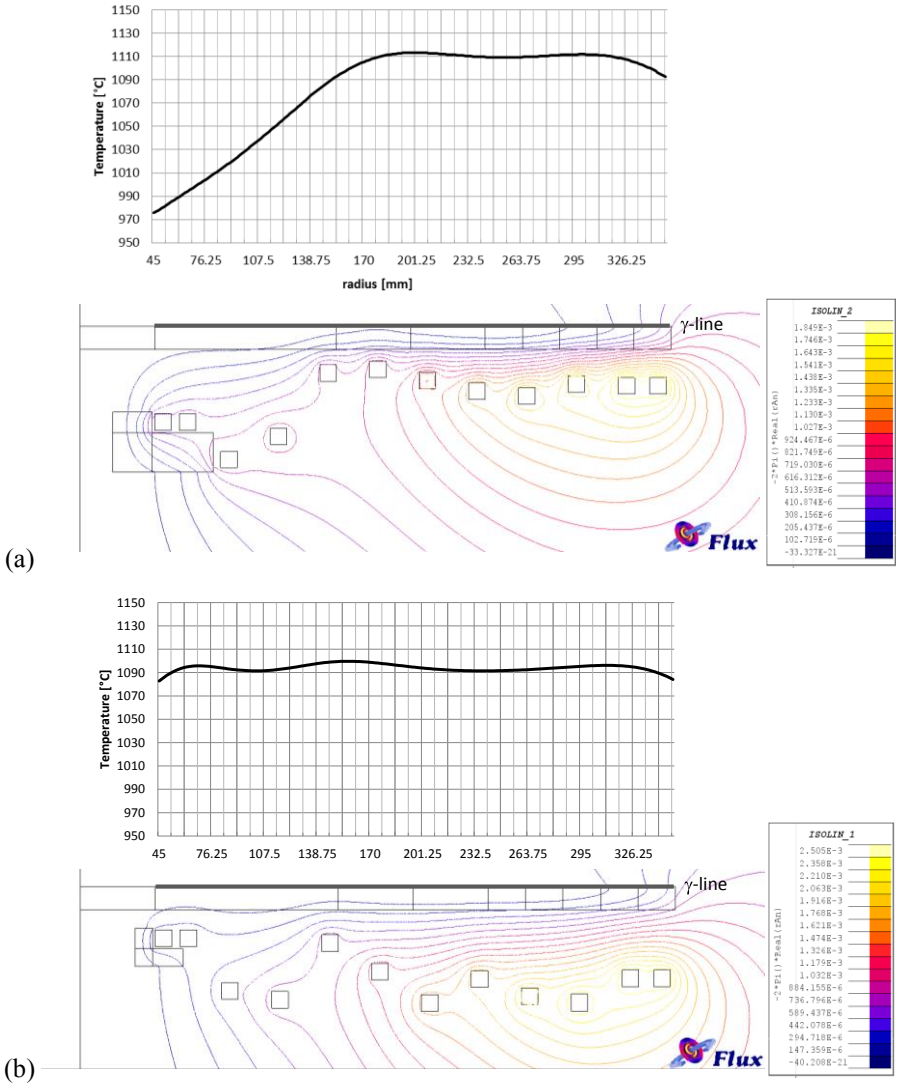

Figure 7 Geometry, magnetic flux lines and temperature on the disk surface of two solutions on Pareto front obtained using NSGA-II algorithm. (a) Point N1 and (b) point N2.

Table 4: turn positions [mm], ferrite sizes [mm] and values of objective functions (6) and (7) for solutions highlighted in Figure 6.

	h_1	h_2	h_3	h_4	h_5	h_6	h_7	h_8	h_9	h_{10}	h_f	L_f	f_1	f_2
N1	28.3	5.6	19.6	57.9	60.0	53.2	47.0	44.1	51.1	50.1	23.8	37.0	0.058	107
N2	55.6	23.9	18.6	52.6	35.5	16.8	31.0	20.9	17.0	31.6	10.5	18.3	0.072	53
M1	46.2	45.9	59.7	52.1	40.9	53.7	26.0	49.7	58.0	59.6	14.7	5.4	0.055	130
M2	55.6	24.1	21.3	49.9	32.4	22.4	32.1	22.0	14.8	32.2	11.1	21.7	0.071	36

Comparing Figure 7(b) and 8(b), that correspond to the points M2 and N2 in Figure 6 for which (7) is minimum, it is evident that the found solutions in terms of turns positions and ferrite sizes are very similar, as well as it appears in Table 4. In contrast, the geometry in Figure 7 (a) and 7(b) are very different in terms of both ferrite sizes and turn positions.

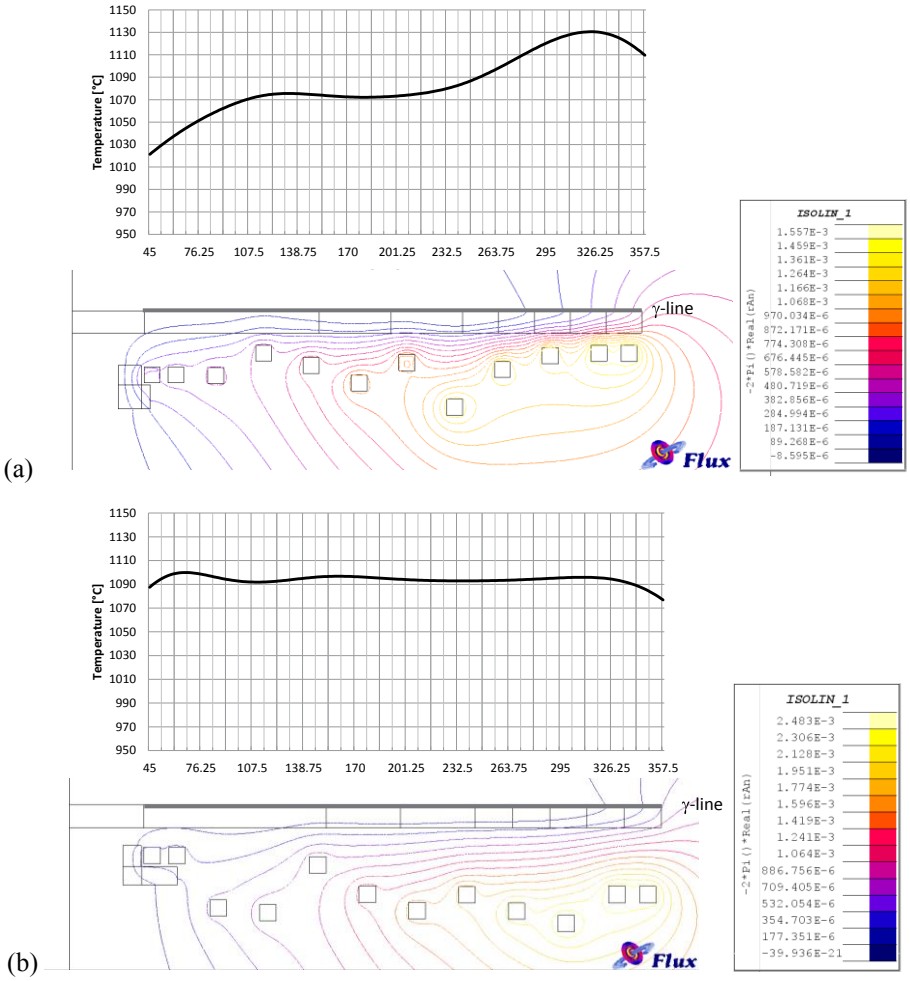

Figure 8 Geometry, magnetic flux lines and temperature on the disk surface of two solutions on Pareto front obtained using MNSGA algorithm. (a) Point M1 and (b) point M2.

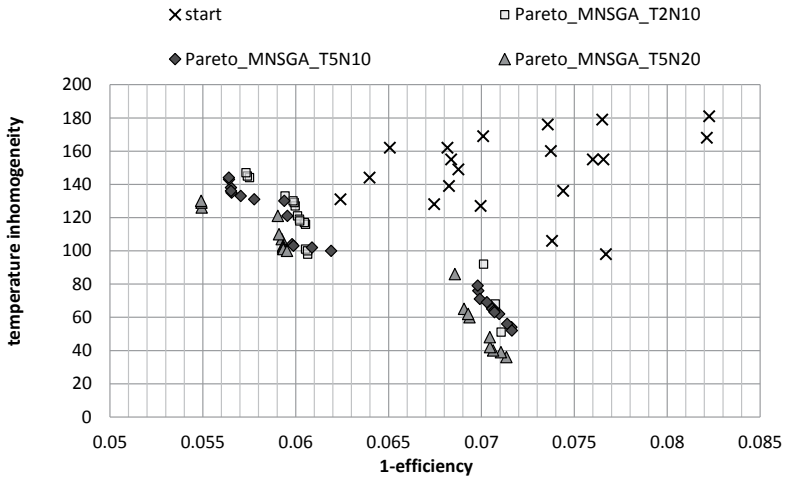

Figure 9 Comparison of the Pareto fronts obtained using MNSGA with different set-up of the immigration parameters (as in Table 3).

Figure 9 shows the Pareto front obtained starting from the same initial population and tuning the MNSGA algorithm as in Table 3: a different tuning of the optimization algorithm gives rise to different approximated Pareto fronts.

4. CONCLUSIONS

The paper shows the results obtained solving a multi-physics benchmark problem and optimizing two objectives functions stemming from two different physical domains. The approximated Pareto fronts prove a substantial improvement of the objective functions with respect to the initial sets. In particular, optimal solutions with very good temperature uniformity have been found.

REFERENCES

[1] Di Barba P, Dughiero F, Lupi S, Savini A. Optimal shape design of devices and systems for induction-heating: Methodologies and applications. *COMPEL - Int J Comput Math Electr Electron Eng* (2003) **22**:111–22.

[2] Di Barba P, Forzan M, Sieni E. Multi-objective design of a power inductor: a benchmark problem of inverse induction heating. *COMPEL - Int J Comput Math Electr Electron Eng* (2014) **33**:1990–2005.

[3] Di Barba P, Dughiero F, Forzan M, Sieni E. Parametric vs non-parametric optimal design of induction heating devices. *Int J Appl Electromagn Mech* (2014) **44**:193–9.

[4] Di Barba P, Dughiero F, Forzan M, Sieni E. A Paretian Approach to Optimal Design With Uncertainties: Application in Induction Heating. *Magn IEEE Trans On* (2014) **50**:917–20.

[5] Di Barba, P, Pleshivtseva Y, Rapoport E, Forzan M, Lupi S, Sieni E, Nacke B, Nikanorov A, Multi–objective optimisation of induction heating processes: methods of the problem solution and examples based on benchmark model. *Int J Microstruct Mater Prop* (2013) **8**:357–72.

[6] Pleshivtseva Y, Di Barba, P., Rapoport E, Nacke B, Nikanorov A, Lupi S, Sieni E, Forzan, M. Multi-objective optimisation of induction heaters design based on numerical coupled field analysis. *Int J Microstruct Mater Prop* (2014) **9**:532–551.

[7] Forzan, M., Maccalli, G., Valente, G., Crippa, D. Design of an innovative heating process system for the epitaxial growth of silicon carbide layers wafer, *Proc. of MMP-Modelling for Material Processing* (2006):101-107.

[8] Di Barba P. *Multiobjective shape design in electricity and magnetism*. Doredrecht ; New York: Springer; (2010).

[9] Di Barba, Paolo, Forzan M., Sieni E. Multiobjective design optimization of an induction heating device: a benchmark problem. *Int J Appl Electromagn Mech* (in press).

[10] Simon D. Biogeography-Based Optimization. *Evol Comput IEEE Trans On* (2008) **12**:702–13.

[11] Forrest S. Genetic Algorithms: Principles of Natural Selection Applied to Computation. *Science* (1993) **261**:872–8.

[12] Schmitt LM. Theory of genetic algorithms. *Theor Comput Sci* (2001) 259:1–61.

[13] Xu S, Ji Z, Pham DT, Yu F. Binary Bees Algorithm – bioinspiration from the foraging mechanism of honeybees to optimize a multiobjective multidimensional assignment problem. *Eng Optim* (2011) **43**:1141–59.
[14] Dos Santos Coelho L, Alotto P. Electromagnetic Optimization Using a Cultural Self-Organizing Migrating Algorithm Approach Based on Normative Knowledge. *Magn IEEE Trans On* (2009) **45**:1446–9.
[15] Hu X-M, Zhang J, Li Y. Orthogonal Methods Based Ant Colony Search for Solving Continuous Optimization Problems. *J Comput Sci Technol* (2008) **23**:2–18.
[16] Palupi Rini D, Mariyam Shamsuddin S, Sophiyati Yuhaniz S. Particle Swarm Optimization: Technique, System and Challenges. *Int J Comput Appl* (2011) **14**:19–27.
[17] Kennedy J, Eberhart R. Particle swarm optimization. *Neural Netw 1995 Proc IEEE Int Conf On* (1995) **4**:1942–8.
[18] Märtens M, Izzo D. The asynchronous island model and NSGA-II: study of a new migration operator and its performance. *Proc. 15th Annu. Conf. Genet. Evol. Comput., Amsterdam, The Netherlands: ACM*; (2013):1173–80.
[19] Deep K, Dipti. A self-organizing migrating genetic algorithm for constrained optimization. *Appl Math Comput* (2008) **198**:237–50.
[20] Zelinka I. Real-time deterministic chaos control by means of selected evolutionary techniques. *Eng Appl Artif Intell* (2009) **22**:283–97.
[21] Zgraja J. The optimisation of induction heating system based on multiquadric function approximation. *COMPEL - Int J Comput Math Electr Electron Eng* (2005) **24**:305–13.
[22] Forzan M, Lupi S, Toffano E. Compensation of induction heating load edge-effect by space control. *COMPEL - Int J Comput Math Electr Electron Eng* (2011) **30**:1558–69.
[23] FLUX. (CEDRAT): www.cedrat.com/software/flux/flux.html [last visit January 2015].
[24] Di Barba P, Savini A, Wiak S. *Field models in electricity and magnetism*. [Dordrecht]: Springer; (2008).
[25] Aliferov A, Dughiero F, Forzan M. Coupled Magneto-Thermal FEM Model of Direct Heating of Ferromagnetic Bended Tubes. *Magn IEEE Trans On* (2010) **46**:3217–20.
[26] Karban P, Kotlan V, Dolezel I. Numerical Model of Induction Shrink Fits in Monolithic Formulation. *Magn IEEE Trans On* (2012) **48**:315–8..
[27] Carslaw H. *Conduction of heat in solids*. 2nd ed. Oxford [Oxfordshire] New York: Clarendon Press; Oxford University Press; (1986).
[28] Di Barba P, Dughiero F, Sieni E, Candeo A. Coupled Field Synthesis in Magnetic Fluid Hyperthermia. *Magn IEEE Trans On* (2011) **47**:914–7.
[29] Dughiero F, Forzan M, Pozza C, Sieni E. A Translational Coupled Electromagnetic and Thermal Innovative Model for Induction Welding of Tubes. *IEEE Trans Magn* (2012) **48**:483–6.
[30] P. Di Barba,F. Dughiero, M. Forzan, E. Sieni. Sensitivity-based optimal shape design of induction-heating devices. *IET Sci Meas Technol* (in press).
[31] Deb K, Pratap A, Agarwal S, Meyarivan T. A fast and elitist multiobjective genetic algorithm: NSGA-II. *Evol Comput IEEE Trans On* (2002) **6**:182–97.
[32] Deb K. *Multi-objective optimization using evolutionary algorithms*. 1st ed. Chichester ; New York: John Wiley & Sons; (2001).